Chemical Geology 535 (2020) 119454

Contents lists available at ScienceDirect

Chemical Geology

journal homepage: www.elsevier.com/locate/chemgeo

Sulfur isotope ratios in co-occurring barite and carbonate from Eocene sediments: A comparison study

Kotaro Toyama[a,1], Adina Paytan[b], Ken Sawada[c], Takashi Hasegawa[a,*]

[a] Institute of Science and Engineering, Kanazawa University, Kakuma-machi, Kanazawa, Ishikawa 920-1192, Japan
[b] Institute of Marine Sciences, University of California Santa Cruz, Santa Cruz, CA 94064, USA
[c] Department of Earth and Planetary Sciences, Faculty of Science, Hokkaido University, N10W8, Kita-ku, Sapporo 060-0810, Japan

ARTICLE INFO

Editor: Michael E. Böttcher

Keywords:
Sulfur isotope
Carbonate associated sulfate
Barite
Eocene
Equatorial Pacific Ocean

ABSTRACT

In order to investigate the utility of bulk carbonate as a recorder of seawater sulfate sulfur isotope ratios ($\delta^{34}S_{sw}$), co-existing pelagic barite and bulk carbonate in Eocene sediments from the Equatorial Pacific Ocean (IODP Exp. 320/321 Sites U1331 to U1333) were analyzed for their sulfur isotope ratios ($\delta^{34}S$). The $\delta^{34}S$ from both minerals showed parallel fluctuation throughout the Eocene with carbonate associated sulfate (CAS) values about 0.8‰ heavier than those of barite. A similar offset was observed in CAS $\delta^{34}S$ obtained using species-specific cleaned planktonic foraminifers in a previous study. The consistent results from two distinct minerals suggest that the original $\delta^{34}S_{sw}$ can be derived from bulk CAS analysis, if post deposition carbonate recrystallization is minimal.

The combined data set showed a ~5‰ increase of $\delta^{34}S_{sw}$ during the Eocene (from 53 Ma to 36 Ma) with the majority of the shift within 7 myr between 53 and 46 Ma. This change is more gradual than previously reported. The timing of this $\delta^{34}S_{sw}$ shift coincides with extensive pyrite burial in the Arctic Ocean, supporting the hypothesis that the 5‰ increase in Eocene $\delta^{34}S_{sw}$ has been caused by ^{34}S-enriched water outflow from the Arctic Ocean.

1. Introduction

The sulfur isotopic composition of sulfate dissolved in seawater ($\delta^{34}S_{sw}$) is a fundamental parameter for the quantification of fluxes in the coupled global sulfur–carbon–oxygen–metal cycles (Schidlowski et al., 1983; Garrels and Lerman, 1984; Holland, 2002; Bottrell and Newton, 2006; Böttcher et al., 2007). The marine sulfur cycle over geologic timescales is closely linked to the redox state of the Earth's surface environments due to the burial of redox-sensitive sulfur species (i.e. sulfide and sulfate) (Berner and Raiswell, 1983). Fluctuations in the $\delta^{34}S_{sw}$ record have been related to a wide range of global environmental changes, such as oxygenation of the atmosphere, bacterial evolution, and mass extinctions (Bottrell and Newton, 2006; Gill et al., 2011; Fike and Grotzinger, 2008). Temporal records of $\delta^{34}S_{sw}$ have been reconstructed using evaporites, pelagic barite and the sulfate in carbonate minerals (Claypool et al., 1980; Strauss, 1997; Kampschulte and Strauss, 2004; Paytan et al., 1998, 2004; Present et al., 2015; Markovic et al., 2016; Yao et al., 2018; Rennie et al., 2018; Yao et al., 2019; Yao et al., 2020).

Several studies have shown relatively rapid changes in the Phanerozoic $\delta^{34}S_{sw}$ record (Paytan et al., 1998, 2004; Fike and Grotzinger, 2008; Gill et al., 2011; Rose et al., 2019a). Such rapid changes are not expected because the oceanic residence time of dissolved sulfate exceeds 10 myr (Claypool et al., 1980; Walker, 1986). For example, Fike and Grotzinger (2008) reported that $\delta^{34}S_{sw}$ derived from bulk carbonate rocks from the Ediacaran–Cambrian boundary (547 to 540 Ma) in the Ara Group, Oman, increased from 20‰ to 42‰ over 7 myr. They suggested that this $\delta^{34}S_{sw}$ shift was caused by a significant increase in primary pyrite formation in nutrient-rich water, accompanied by increased sequestering efficiency of organic carbon by biological packaging and/or increased sedimentation rates. Gill et al. (2011) estimated that the $\delta^{34}S_{sw}$ during the Toarcian Oceanic Anoxic Event in the Early Jurassic (183 to 179 Ma) increased from 17‰ to 23‰, based on $\delta^{34}S$ data of calcitic belemnite guards from northeast England and bulk carbonate rocks from southern Italy. They concluded that this positive $\delta^{34}S_{sw}$ shift can be generated by transiently increasing the burial rate of pyrite under euxinic (i.e., anoxic and sulfidic) conditions in the water column. Paytan et al., (1998) reported a 5‰ increase (from 17‰ to 22‰) in $\delta^{34}S_{sw}$ values for the early Eocene (53 to 45 Ma) obtained from pelagic barite ($\delta^{34}S_{barite}$) from several oceanic

* Corresponding author.
E-mail address: jh7ujr@staff.kanazawa-u.ac.jp (T. Hasegawa).
[1] Present affiliation: Graduate School of Science and Liberal Arts, The University of Tokyo.

https://doi.org/10.1016/j.chemgeo.2019.119454
Received 27 May 2019; Received in revised form 25 December 2019; Accepted 26 December 2019
Available online 08 January 2020

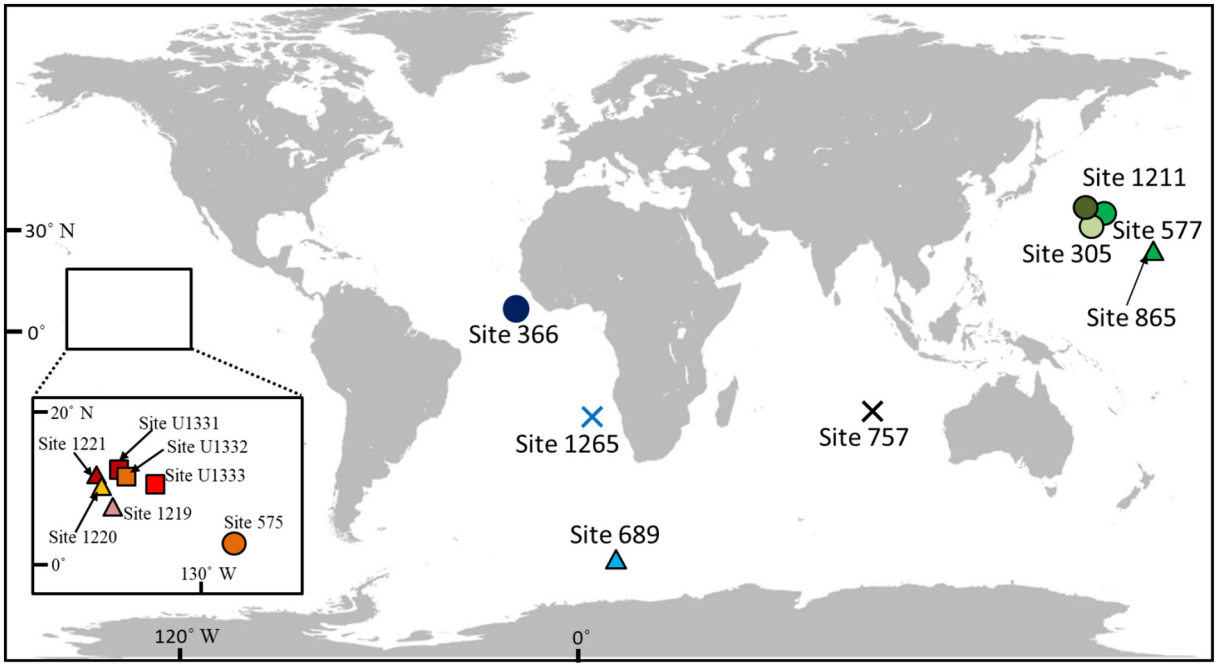

Fig. 1. Map showing sample sites of the present and previous studies. The locations of Sites 1219 to 1221, Site 689, Site 575, Site 577, Site 865, Site 305, Site 1211, Site 366, Site 1265 and Site 757 are from Lyle et al. (2002), Barker et al. (1988), Mayer et al. (1985), Heath et al. (1985), Sager et al. (1993), Moberly et al. (1975), Bralower et al. (2002), Lancelot et al. (1978), Zachos et al. (2004) and Peirce et al. (1989), respectively.

sediments cores. Several interpretations were suggested by different researchers for the driver of this $\delta^{34}S_{sw}$ shift including: the dissolution of basin scale evaporites with high $\delta^{34}S$ values (Wortmann and Paytan, 2012); pyrite burial under euxinic environments in epicontinental seas (Kurtz et al., 2003) or in the ocean (Rennie et al., 2018); or local pyrite burial in the Arctic Ocean (Ogawa et al., 2009). However, the exact mechanism of the $\delta^{34}S_{sw}$ shift in the Eocene remains unclear.

Pelagic barite is an excellent mineral for reconstructing $\delta^{34}S_{sw}$, because of the negligible sulfur isotope fractionation (< 0.4‰) associated with its precipitation (Paytan et al., 1998; Ganeshram et al., 2003; Paytan and Griffith, 2007) and due to the low solubility of barite at normal marine temperature and pH conditions. Moreover, barite is stable during diagenesis as long as dissolved sulfate is not depleted in the pore water (Dean and Schreiber, 1977; Dymond et al., 1992; Paytan et al., 1993; Paytan et al., 2002). However, barite is only abundant in areas of relatively high export production in the open ocean (Paytan et al., 1996). Therefore, pelagic barite is not found in all sediments limiting its use for the reconstruction of $\delta^{34}S_{sw}$.

Carbonate associated sulfate (CAS), on the other hand, can be extracted from most carbonate rocks which are widespread and abundant in the geological record. CAS has been used to reconstruct $\delta^{34}S_{sw}$ (Takano, 1985; Kampschulte and Strauss, 2004; Perrin et al., 2017; Rennie et al., 2018). Burdett et al. (1989) and Kampschulte and Strauss (2004) reported that the $\delta^{34}S$ of CAS ($\delta^{34}S_{CAS}$) (21.2 ± 0.8‰) obtained from various modern biogenic carbonates (bivalves, brachiopods, gastropods, foraminifers, etc.) is similar to that of the seawater (20.9 ± 0.5‰) in which their skeletons were formed (Kampschulte et al., 2001; Longinelli, 1989). However, it has been pointed out that when using CAS special attention should be paid to ensure the accuracy of the record, because $\delta^{34}S_{CAS}$ is susceptible to diagenetic overprinting (Turchyn et al., 2009; Rennie and Turchyn, 2014). Sulfate reduction in sediments increases the $\delta^{34}S$ value of pore water sulfate and this ^{34}S-enriched sulfate could be incorporated into calcite that is precipitated as secondary crystals in the sediments, obscuring the original CAS value (Pierre, 1985; Habicht and Canfield, 1997; Kampschulte and Strauss, 2004).

To investigate the utility of CAS as an archive for $\delta^{34}S_{sw}$, Rennie and Turchyn (2014) analyzed bulk carbonates in calcareous sediments (i.e., foraminifera and calcareous nannoplankton ooze) from several pelagic ocean sites for the last 25 myr and reported that most of the $\delta^{34}S_{CAS}$ data were about 2‰ higher than the coeval barite data previously published by Paytan et al. (1998). They suggested that this discrepancy reflected the effect of diagenetic overprinting during carbonate recrystallisation. Recently Rennie et al. (2018) compared $\delta^{34}S_{CAS}$ obtained from single foraminiferal tests corrected for species specific offsets from seawater to the previously published Eocene $\delta^{34}S_{barite}$ (Paytan and Gray, 2012). They obtained a similar trend with about 1‰ offset between the records ($\delta^{34}S_{CAS}$ 1‰ higher than $\delta^{34}S_{barite}$). The offset was attributed to S isotope fractionation during precipitation of one or both of these phases (Rennie et al., 2018). It should be noted, however, that these previous studies compared the $\delta^{34}S$ values of CAS and barite derived from *different* ODP/IODP sites. This prevents direct comparison between the $\delta^{34}S$ values of the two phases at the exact same age and burial site.

Here we report for the first time $\delta^{34}S$ values of co-occurring pelagic barite and CAS extracted from the same sediment samples from Equatorial Pacific IODP Exp. 320/321, spanning the age between 30 and 52 Ma. The potential use of bulk carbonate-extracted CAS as a tool for high resolution $\delta^{34}S_{sw}$ reconstruction is discussed based on these data.

2. Methods

2.1. Samples and experimental methods

Eocene and Oligocene sediments (52–30 Ma) from Sites U1331, U1332 and U1333 from the eastern Equatorial Pacific Ocean (Fig. 1 and Table 1) recovered by IODP Exp. 320/321 were used in this study (see also Pälike et al., 2010). We used “squeezed cakes”, the residues after on-board extraction of interstitial water (Pälike et al., 2010). Coexisting CAS and barite in each sample were extracted by combining the methods of Burdett et al. (1989) and Paytan et al. (1993) as described below. Vacuum-dried samples (10–30 g) were immersed overnight in deionized (DI) water to remove any soluble sulfate. The samples were

Table 1
Sample information and $\delta^{34}S$ of the extracted barite and CAS.

Site	Hole	Core	Section	Section interval (cm)	Core depth (mbsf)	Age[a] (Ma)	Carbonate content (%)	$\delta^{34}S_{barite}$ (‰, VCDT)	$\delta^{34}S_{CAS}$ (‰, VCDT)	SO_4^{2-} concentration in pore water[b] (mM)
U1331	A	3H	2	145–150	17.7	31.2	90	21.7	21.7	27.9
U1331	A	10H	3	145–150	85.7	41.4	40	n.e.	22.4	27.7
U1331	A	17X	3	145–150	152.1	46.4	11	n.e.	21.3	27.5
U1331	A	19X	2	19–29	161.8	48.3	13	n.e.	19.8	
U1331	B	17H	1	140–150	154.1	46.6	10	n.e.	22.0	30.2
U1331	C	16H	3	111–121	181.2	51.2	13	n.e.	18.2	
U1331	C	17H	2	50–60	186.1	51.7	10	n.e.	18.6	
U1332	A	9H	2	145–150	73.4	33.4	91	n.e.	21.7	
U1332	A	14H	3	145–150	122.4	42.1	43	n.e.	22.3	27.0
U1332	A	15X	3	140–150	130.4	43.7	43	n.e.	21.9	26.1
U1333	A	14X	3	140–150	124.5	36.4	54	22.0	22.8	26.9
U1333	A	16X	3	140–150	143.7	40.2	13	n.e.	22.3	26.1
U1333	A	17X	2	0–10	150.4	41.1	n.d.	21.4	22.3	
U1333	A	17X	3	140–150	153.3	41.4	69	n.e.	21.9	25.7
U1333	A	17X	4	140–150	154.8	41.6	n.d.	21.4	22.4	
U1333	A	17X	5	107–117	155.9	41.9	n.d.	21.7	22.4	
U1333	A	18X	1	140–150	159.9	42.5	53	n.e.	21.9	27.0
U1333	A	18X	3	115–125	161.9	43.1	n.d.	21.3	22.2	
U1333	A	19X	1	111–121	169.2	44.6	54	21.0	21.9	
U1333	A	19X	2	140–150	170.7	45.0	12	n.e.	21.7	25.5
U1333	A	19X	5	13–23	174.2	45.7	90	21.0	22.1	
U1333	A	20X	1	130–140	179.0	46.8	85	20.6	21.7	
U1333	B	19X	3	10–20	165.9	43.9	49	n.e.	21.9	
U1333	B	19X	5	22–32	169.0	44.6	78	21.5	22.1	
U1333	B	20X	1	41–51	172.8	45.4	91	21.5	22.0	
U1333	B	20X	2	90–100	174.6	45.8	83	21.6	22.1	

n.e.: not extracted.
n.d.: no data.
[a] The ages were corrected according to Gradstein et al. (2012).
[b] Data from Pälike et al. (2010). Only data taken from identical samples with our analyses are shown.

sieved and the coarse fraction (> 125 μm) was used for picking benthic foraminifera which were used for oxygen isotope analyses. The residual coarse fraction sample (after the benthic foraminifers were picked) was mixed with the fine fraction and the combined sediment was treated with a 5% NaClO solution overnight to remove organic matter. The supernatant was separated using centrifugation and discarded, and the residue was rinsed three times with DI water and dried. The dried residue was weighed and treated with 0.5 M HCl solution overnight to dissolve the carbonate. The supernatant was filtered using a 0.20 μm polycarbonate filter, and 10 mL of 0.5 M $BaCl_2$ solution was added and left to precipitate for 3 days at 60 °C to recover CAS as $BaSO_4$. The use of excess $BaCl_2$ ensures complete scavenging of the sulfate associated with the carbonate as barite. The residual sample was rinsed three times with DI water and treated with 6 M HCl overnight at room temperature to remove HCl soluble materials such as pyrite. After that we followed the barite separation procedure as described in Paytan et al. (1993).

2.2. Analytical methods

The carbonate content in the samples was estimated by weight difference following the 0.5 M HCl treatment. The chemical composition of each barite extraction sample was checked using a scanning electron microscope with energy dispersive X-ray spectroscopy (SEM-EDX, HITACHI SEM-EDX TypeN). Images of barite crystals and foraminiferal tests were taken using a field emission scanning electron microscope system (FE-SEM, JEOL JCM-6010LV).

For $\delta^{34}S$ measurements of barite precipitated from the CAS and marine barite extracted from sediments, about 0.22 mg barite was weighted into a tin capsule and 1.2 mg V_2O_5 was added. The samples were combusted in an ANCA-SL elemental analyzer and introduced as SO into a Sercon 20-22 gas source mass spectrometer at the Paleo-laboratory of Kanazawa University. Elemental analyzer settings for the furnace and GC were 1080 °C and 50 °C, respectively. The isotope value expressed in δ-notation relative to the VCDT (Vienna Canyon Diablo Troilite, Halas and Szaran, 2001) standard is defined as:

$$\delta^{34}S\ (‰) = \left\{ \frac{(^{34}S/^{32}S)_{Sample} - (^{34}S/^{32}S)_{VCDT}}{(^{34}S/^{32}S)_{VCDT}} \right\} \times 1000$$

The measurements were calibrated using international standards NBS127 (+21.1‰ vs. VCDT, Coplen et al., 2002), IAEA-S-2 (+22.6‰ vs. VCDT, Taylor et al., 2000) and IAEA-SO-5 (+0.5‰ vs. VCDT, Halas and Szaran, 2001). The repeated measurement of NBS127 during the analyses showed that the instrumental reproducibility was within 0.3‰.

3. Results

The carbonate contents in the sediment samples, which are shown in Table 1, range from 10% to 91%. Barite was extracted from 12 of the 26 samples. No barite could be obtained from Site U1332. The SEM image of the barite extraction residue from U1333A 19X-5 13–23 cm is shown in Fig. 2A. The crystals were identified as pelagic barite based on their morphology with euhedral and ellipsoidal shapes ranging in size from 2 to 5 μm. Larger diagenetic barite with tabular-shaped crystals (Torres et al., 1996; Paytan et al., 2002) was not observed in any of our samples.

The $\delta^{34}S$ values of the barite and coexisting CAS samples are shown in Table 1 and plotted in Fig. 3A against the geologic time scale of Gradstein et al. (2012). Each of $\delta^{34}S$ values (for CAS and barite) represents an average of three measurements and each error bar indicates the standard deviation (1σ) of the triplicated analysis of each sample. The $\delta^{34}S_{barite}$ values of samples U1331A 3H-2 and U1333B 19X-5 and their associated errors were determined from two measurements due to the small amount of barite obtained from these samples. The lowest $\delta^{34}S_{barite}$ value (20.6‰) was obtained from sample U1333A 20X-1 130–140 cm with an assigned age of 46.8 Ma in the middle Eocene

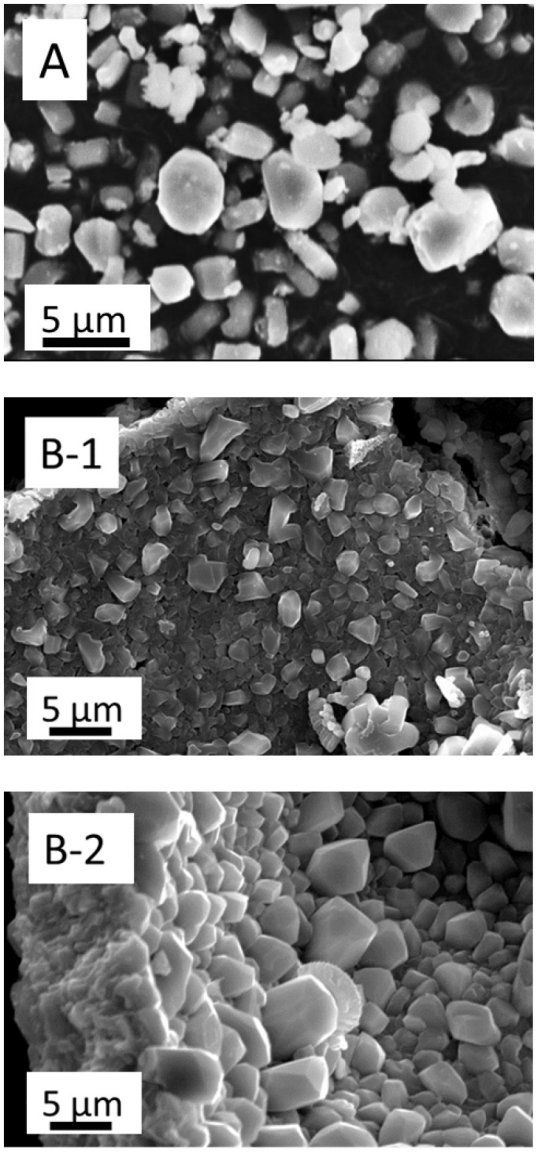

Fig. 2. SEM images of (A) pelagic barite from U1333A 19X-5 13–23 cm and (B) internal wall of the foraminiferal tests in the sediment samples. B-1 is from U1333A 14X-3 140–150 cm, and B-2 is from U1333B 19X-5 22–32 cm, respectively. Recrystallized calcite is observed on the wall of the foraminiferal tests.

(Lutetian, 47.8 to 41.2 Ma). The barite samples above this horizon in U1333 showed a gradual increase of the $\delta^{34}S_{barite}$ toward 22.0‰ along with the stratigraphic level (Fig. 3A). The sample that recorded the highest $\delta^{34}S_{barite}$ value (22.0‰) was U1333A 14X-3 140–150 cm with an age of 36.4 Ma in the late Eocene (Priabonian, 37.8 to 33.9 Ma). A sample extracted from U1331A 3H-2 145–150 cm with an age of 31.2 Ma, in the lower Oligocene (Rupelian, 33.9 to 28.1 Ma), had a $\delta^{34}S_{barite}$ value of 21.7‰, similar to that of the sample at 36.4 Ma.

Twenty-six CAS samples from U1331, U1332 and U1333 were analyzed and the $\delta^{34}S_{CAS}$ values exhibited a 3.5‰ shift from 18.2 to 21.7‰ within 5 myr between 51.2 and 46.8 Ma (Fig. 3A). A similar shift has been previously reported for barite as well (Paytan et al., 1998; Yao et al., 2020). The $\delta^{34}S_{CAS}$ values over the next 10 myr from 46.8 to 36.4 Ma showed a gradual ~1‰ increase from 21.7 to 22.8‰. The values then dropped by ~1‰ from 22.8 to 21.7‰ between 36.4 and 33.4 Ma and remained the same until 31.2 Ma. The $\delta^{34}S_{CAS}$ values from Site U1333 were slightly higher (ca. 0.8‰) relative to those of co-existing barite (Fig. 3B). One sample analyzed for $\delta^{34}S_{CAS}$ from Site

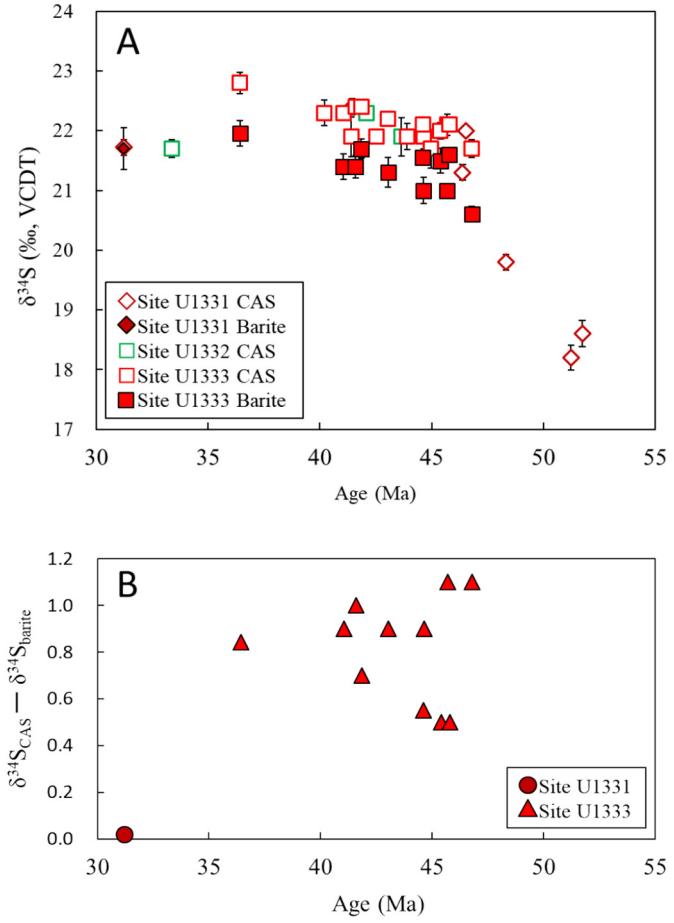

Fig. 3. Sulfur isotope compositions of the barite and CAS obtained from Sites U1331 and U1333 in this study (A), and offset of the $\delta^{34}S$ values of the barite and CAS from each sample (B). The ages of the samples were corrected in accordance with Gradstein et al. (2012). The $\delta^{34}S$ values and error bars are average and the standard deviation (1σ) of triplicated measurements respectively, except for two horizons where only two data points are available. The $\delta^{34}S_{barite}$ values and associated errors of U1331A 3H-2 and U1333B 19X-5 are determined from duplicated measurement due to shortage of barite.

U1331A (i.e., U1331A 3H-2 145–150 cm) showed a value close to that of the coexisting barite. No correlation between the carbonate content and the $\delta^{34}S_{CAS}$ was detected.

4. Discussions

4.1. Bulk carbonate CAS as a proxy for sulfate sulfur isotope ratios in paleo-seawater

It was previously suggested that in the process of dissolution of carbonates for $\delta^{34}S_{CAS}$ analyses contamination from non-CAS sulfur can compromise the data. Specifically, Wotte et al. (2012) argued that the oxidative leaching steps tend to contaminate CAS by partially oxidizing reduced sulfur phases. Sulfate from pyrite oxidation could cause contamination of the sulfate liberated from CAS during the acid dissolution process, and corresponding change in the sulfate isotope composition assigned to the CAS fraction (Marenco et al., 2008; Mazumdar et al., 2008). Therefore, Wotte et al. (2012) extracted CAS using 0.3 M HCl following the NaCl solution treatment without the NaOCl solution treatment. Our samples were treated with NaOCl solution to remove organic matter after the DI water rinses and then extracted for CAS using 0.5 M HCl. If pyrite oxidation affected the $\delta^{34}S_{CAS}$ of our samples we would expect the values to be lower than coeval $\delta^{34}S_{barite}$ (Turchyn

et al., 2009; Rennie and Turchyn, 2014). However, the $\delta^{34}S_{CAS}$ value in the present study was always higher than the coexisting $\delta^{34}S_{barite}$ (Fig. 3A), thus we conclude that the contribution of sulfate derived from pyrite oxidation to the extracted CAS was negligible. We also rule out any sulfur isotope fractionation during precipitation of dissolved CAS as barite because all the sulfate released from the CAS was precipitated as barite, hence fractionation cannot occur (Rennie and Turchyn, 2014).

Rennie and Turchyn (2014) reported $\delta^{34}S$ values obtained from bulk sediments of nannoplankton ooze and from dissolved pore water sulfate for the last 25 myr in several pelagic ocean sites (i.e., ODP Sites 807, 821 and 1003). They reported an increasing trend in pore water $\delta^{34}S$ values (e.g., Site 807) from 20 to 30‰ along with a gradual drop of sulfate ion concentration, from 28 to 22 mM. Enrichment of pore water sulfate in ^{34}S by bacterial sulfate reduction was proposed as a causal mechanism of this observation (Pierre, 1985; Habicht and Canfield, 1997; Kampschulte and Strauss, 2004). The $\delta^{34}S_{CAS}$ values in these studies showed an increasing trend along with the increase in $\delta^{34}S$ value of pore water sulfate. Rennie and Turchyn (2014) suggested that the $\delta^{34}S_{CAS}$ values of the original CAS have been impacted by carbonate dissolution and recrystallization in pore fluids impacted by bacterial sulfate reduction.

As for our samples, Pälike et al. (2010), who used microscopic observations, reported that the Eocene sediments from Sites U1331 to U1333 containing only a small amount of non-biogenic calcite (< 5%). Recrystallized carbonate crystals were observed on the internal wall of foraminiferal tests in these samples (Fig. 2B). The non-biogenic carbonate was interpreted to be formed through diagenetic processes during burial in the sediments. Accordingly, it is likely that the $\delta^{34}S_{CAS}$ value of the recrystallized calcite reflects that of the sulfate in pore-water that was potentially modified from contemporaneous seawater by sulfate reduction. The sulfate concentration of diagenetically recrystallized carbonate (0.5 to 600 ppm, Staudt and Schoonen, 1995; Rose et al., 2019b; Richardson et al., 2019) is low relative to that in foraminiferal tests or in coccoliths (600 to 1000 ppm, Staudt and Schoonen, 1995). Thus, the altered sulfur isotopic signals associated with calcite recrystallization on the bulk carbonate in our samples is likely negligible. However, the effects of recrystallization on $\delta^{34}S_{CAS}$ values have to be carefully assessed for each site based on petrographic inspections of the sediment samples and pore water chemistry.

Sulfate concentrations generally decrease and $\delta^{34}S$ values of sulfate in pore waters increase with depth under condition of bacterial sulfate reduction (Pierre, 1985). This is because microbial redox processes preferentially break the ^{32}S—O bond and the liberated ^{32}S is fixed and removed as pyrite, leaving the residual sulfate pool enriched in ^{34}S (Chambers and Trudinger, 1979). The sulfate concentration of pore water at our study sites does not vary significantly throughout the sediment core (27.5 to 29 mM in Site U1331 and 27.5 to 26 mM in Site U1333, Pälike et al., 2010; see Table 1) suggesting minimal sulfate reduction. The sulfate concentration of Eocene seawater is estimated to be ca. 14 mM (Horita et al., 2002: significantly lower than ca. 28 mM, the present value). The constant and high sulfate concentration in the pore water at our sites is a consequence of diffusion and penetration of "younger seawater" into the sediment (Richter and Liang, 1993; Edgar et al., 2013; Voigt et al., 2015). The source of the pore water is seawater that is "younger" than the associated sediment at each depth. For example, seawater that started penetrating downward during Miocene can reach the Oligocene sediments as pore water. Assuming that this diffusive mixing occurred in the pore water from the Eocene through the present day at the sites, oxic conditions of the pore water have been maintained leading to preservation of pelagic barite and inhibition of pyrite formation. Although the $\delta^{34}S$ of sulfate in the recrystallized calcite reflects the value of the "younger seawater" the amount of non-biogenic calcite in our sample is < 5% (Pälike et al., 2010) hence the effect on the bulk $\delta^{34}S_{CAS}$ values in our samples is expected to be negligible.

As shown in Fig. 3B, the $\delta^{34}S_{CAS}$ values are consistently 0.5–1.1‰ higher than $\delta^{34}S_{barite}$ of the same age without any temporal trend in the offset (except for one sample from Site U1331 that has an identical $\delta^{34}S$ value to barite). The $\delta^{34}S_{CAS}$ offset from $\delta^{34}S_{barite}$ seen in our record is similar to that discussed for planktonic foraminifera (Rennie et al., 2018). Thus, we conclude that the overall $\delta^{34}S_{CAS}$ values obtained here have not been significantly impacted by sulfate reduction and diagenetic carbonate formation and have retained their original signals.

In conclusion we stress that in order to establish sulfur isotope stratigraphy using CAS from marine sediments one must ensure that the $\delta^{34}S_{CAS}$ signal is not impacted by pore water sulfate. Pore water trends that do not show a decrease in sulfate concentrations and/or an increase in $\delta^{34}S$ of sulfate as well as microscopic observations of the carbonate minerals should be used to ensure low content of recrystallized calcite. It is also beneficial to compare the $\delta^{34}S_{CAS}$ with coeval $\delta^{34}S_{barite}$ values from the identical sample if available. Accordingly, the $\delta^{34}S_{CAS}$ of bulk marine carbonate can be used to reconstruct ancient marine sulfate $\delta^{34}S$ with high temporal-spatial resolution because of the widespread occurrence and high abundance of carbonates in the geological record. With careful sample selection sulfur isotope data based on CAS can contribute to reconstruction of climatic and tectonic perturbations that impacted the global biogeochemical sulfur cycle through geological time.

4.2. $\delta^{34}S$ temporal variation in the Eocene

The $\delta^{34}S_{CAS}$ and $\delta^{34}S_{barite}$ values obtained in the present study are shown in Fig. 4 along with the data from previous studies. Our $\delta^{34}S_{CAS}$ values are generally consistent with those from the Atlantic (Site 1265) and Indian Ocean (Site 757) sites reported in Rennie et al. (2018). The $\delta^{34}S_{barite}$ values from the Pacific (Sites 1219 to 1221 and 865) and the Antarctic (Site 689) also exhibit concordant distribution with our $\delta^{34}S_{barite}$ data, while the $\delta^{34}S_{barite}$ data from the Equatorial Atlantic (Site 366; Paytan et al., 1998) through the age interval between 47 and 40 Ma have values elevated by ~1‰. Recently Yao et al. (2020) reported the discrepancy in the $\delta^{34}S_{barite}$ trend from Site 366 and the $\delta^{34}S_{barite}$ from other sites between 53 Ma to 40 Ma. They concluded that these specific barite samples from Site 366 were altered during

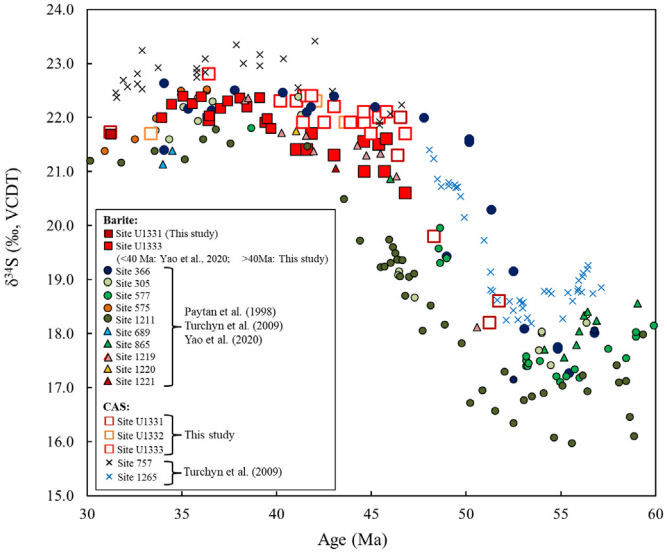

Fig. 4. Secular variation of $\delta^{34}S_{CAS}$ and $\delta^{34}S_{barite}$. Data sets include the present study and previous studies through the Paleogene. The $\delta^{34}S_{barite}$ in Turchyn et al. (2009) was corrected using 21.1‰ as the value of NBS127. The locations of sites in the legend are shown in Fig. 1. The ages of all samples were corrected in accordance with Gradstein et al. (2012). For Site U1333 (red square), 14 data points from < 40 Ma published in Yao et al. (2020) are also shown in addition to the present study. (For interpretation of the references to color in this figure legend, the reader is referred to the web version of this article.)

diagenesis, because the $^{87}Sr/^{86}Sr$ ratios of these barite samples were anomalously high, suggesting incorporation of additional radiogenic Sr from pore water into the barite crystal lattice. Yao et al. (2020) also discussed the process of diagenetic formation of barite and the associated elevated $\delta^{34}S_{barite}$ values for Site 366. To recap here, sulfate depletion by microbial sulfate reduction in pore water leads to dissolution of barite and release of Ba into solution. Since microbial redox processes preferentially break the ^{32}S–O bond in sulfate, and the reduced sulfur precipitates as pyrite (Chambers and Trudinger, 1979), the pore water gradually become enriched in ^{34}S relative to seawater (e.g., Kaplan et al., 1963). These processes lead to high Ba concentration coincided with sulfate depletion with elevated $\delta^{34}S$ of sulfate in the pore water. This fluid can migrate in the sedimentary column (Torres et al., 1996) until it interacts with sulfate-rich "fresh" pore water, which is not affected by microbial sulfate reduction (Torres et al., 1996; Breheret and Brumsack, 2000), and subsequently precipitates so-called diagenetic barite (Paytan et al., 2002). The sulfate in the pore water from which the diagenetic barite precipitates is a mixture of the ^{34}S–enriched residual sulfate that diffused upwards from the sulfate reduction zone and sulfate that is penetrated from above which is not impacted by sulfate reduction. Indeed, it is known that these diagenetic fronts are formed above the sulfate depletion zone (Torres et al., 1996; Breheret and Brumsack, 2000). Thus diagenetic barite can record $\delta^{34}S$ values enriched in ^{34}S to various degrees relative to contemporaneous seawater sulfate depending on the specific proportion of sulfate sources in the pore fluids (Paytan et al., 2002). This can explain the higher $\delta^{34}S_{barite}$ values of Site 366 samples between 47 Ma and 40 Ma relative to the samples from Sites 1331 and 1333.

Our $\delta^{34}S_{barite}$ data from Sites U1331 and U1333 added important $\delta^{34}S_{sw}$ data in the Lutetian. Although three previous studies presented data sets from different regions in this time interval, theyshowed discrepancies between the data sets (Paytan et al., 1998; Turchyn et al., 2009; Yao et al., 2020; Fig. 4). The present study has refined the trend of $\delta^{34}S_{sw}$ during early Eocene (from 46 Ma to 31 Ma) by robust barite data. Establishing the rate of change over this time interval is important for the reconstruction of the paleo-environmental changes that caused the $\delta^{34}S_{sw}$ shift. The data from CAS and barite showed the same trends with an offset between the phases as discussed above. Combining these new data with data from previous studies, we see that the $\delta^{34}S_{sw}$ in the Eocene gradually increased by about 5‰ between 53 and 36 Ma with most of the shift within 7 myr between 53 and 46 Ma, consistent with a recent publication (Yao et al., 2020).

Several previous studies provided different explanations for the cause of the +5‰ $\delta^{34}S_{sw}$ shift, we note that all these interpretations are potentially viable because the system is under constrained as outlined by Paytan et al. (1998). Wortmann and Paytan (2012) suggested that the $\delta^{34}S_{sw}$ shift can be ascribed to the dissolution of basin scale evaporite deposits of Neoproterozoic to Early Cambrian age with high $\delta^{34}S$, following the India-Eurasia collision (53.7 to 50.6 Ma: Najman et al., 2010; Clementz et al., 2011) in conjunction with low seawater sulfate concentrations. Kurtz et al. (2003) discussed the cause of the $\delta^{34}S_{sw}$ shift as a pulse of pyrite burial in widespread euxinic environments along inland seas and continental shelves in the wake of the sea-level rise during the early Eocene.

Most recently, Rennie et al. (2018) attributed the shift to changes in depositional depth of pyrite from shallow to deep settings. They concluded that changes in the deposition site of pyrite explained half of the +5‰ shift, whereas the other half was largely ascribed to a rapid change of the average isotope composition of the pyrite that was deposited at ~53 Ma. The idea of the change in the above pyrite burial flux is similar to that of Kurtz et al. (2003) but the site of burial differs. Rennie et al. (2018) suggested that the sea level change associated with the Indian collision with Eurasia was a primary factor that caused the locus shift of pyrite burial from shallow to the deep ocean settings. However, such tectonically driven locus change of pyrite burial and subsequent shift in $\delta^{34}S_{sw}$ values would occur over time scales of 10 myr or more and not likely to be as quick as the shift seen in the data. Independent assessment of pyrite concentrations in open ocean marine sediments across the time interval where the $\delta^{34}S_{sw}$ shift is recorded could be used to verify this interpretation.

Ogawa et al. (2009) provided interesting geologic data that may resolve the enigma of the $\delta^{34}S_{sw}$ shift of the early-middle Eocene. They reported that sedimentary sulfur for the early Eocene in the Arctic Ocean occurred mainly as framboidal pyrite and its $\delta^{34}S$ values ranged around −20‰ at 50 Ma and up to −50‰ at 45 Ma. They further suggested that as an isolated basin the coeval seawater of the Arctic Ocean may have had elevated $\delta^{34}S_{sw}$. They therefore speculated that the discharge of Arctic seawater to the North Atlantic Ocean around 50 Ma could explain a 3‰ increase in $\delta^{34}S_{sw}$. Paleontological, paleogeographic and paleoceanographic studies (Akhmetiev and Beniamovski, 2004; Backman et al., 2006; Gleason et al., 2009; Stickley et al., 2009) indicate seawater exchange between the Arctic ocean and the North Atlantic around this time period.

The refined curve in the present study indicates that the $\delta^{34}S_{sw}$ value in the Eocene gradually increased by about 5‰ between 53 and 36 Ma with the majority of the shift within 7 myr between 53 and 46 Ma, especially around 47 Ma. The timing of the $\delta^{34}S_{sw}$ shift corresponds to the pyrite burial event in the Arctic Ocean. A simple mass balance model used to calculate the magnitude of the $\delta^{34}S_{sw}$ shift that could be associated with the Arctic Ocean water input to the Atlantic was reported by Ogawa et al. (2009). They used the sulfate concentration of present seawater in their model and concluded that the Arctic Ocean input could explain a *fraction* of the $\delta^{34}S$ shift seen in global seawater. On the other hand, if the sulfate concentration in seawater was lower in the early Eocene as suggested by several studies (~14 mM; Horita et al., 2002; Halevy et al., 2012), Arctic outflow water mixed with the rest of the global ocean could explain the entire +5‰ shift. Thus, we believe that our results support the hypothesis of Ogawa et al. (2009) that the early Eocene $\delta^{34}S_{sw}$ shift was caused by the ^{34}S-enriched water outflow from the Arctic Ocean.

5. Summary

The sulfur isotope ratios ($\delta^{34}S$) of co-existing pelagic barite and bulk carbonate in Eocene sediments from the eastern Equatorial Pacific Ocean (IODP Exp. 320/321 Sites U1331-U1333) were determined. The obtained $\delta^{34}S_{CAS}$ values are 0.5–1.1‰ higher than $\delta^{34}S_{barite}$ of the same samples without systematic change in the magnitude of the offset over time. The parallel fluctuation suggests that our $\delta^{34}S_{CAS}$ values are not significantly impacted by including sulfate from diagenetic carbonate that is formed post-burial and was impacted by sulfate reduction but rather these samples retain their original signals. Thus, the bulk $\delta^{34}S_{CAS}$ values from these cores at this age interval are robust for paleoceanographic $\delta^{34}S_{sw}$ reconstruction, although careful evaluation of the pore water chemistry and carbonate preservation are needed when using bulk carbonate CAS at other locations.

Our $\delta^{34}S_{barite}$ data added an important data set in the Lutetian. The refined curve indicates that the $\delta^{34}S_{sw}$ variation of early to middle Eocene gradually increased from 17.5‰ at 53 Ma to about 21.5‰ at 46 Ma. The timing of this $\delta^{34}S$ shift is similar to that of pyrite burial in Arctic Ocean. Mass-balance calculation indicate that the +5‰ evolution of Eocene $\delta^{34}S_{sw}$ could be attributed to the outflow of ^{34}S-enriched water from the Arctic Ocean as suggested in a previous study.

Declaration of competing interest

The authors declare that they have no known competing financial interests or personal relationships that could have appeared to influence the work reported in this paper.

Acknowledgment

The present authors express their deep appreciation to two anonymous reviewers for their constructive comments, Prof. M. Böttcher for his editorial inputs and Dr. A.S. Goto for her great assistance for maintaining the analytical systems in the lab as well as critical discussion. Appreciation is also due to Mr. K. Hasebe and Miss C. Nakase for their discussion on the data. This work was supported by JSPS KAKENHI Grant Numbers 20340144, 24403012 and 26247086 for Hasegawa and NSF award 1821976 for Paytan.

References

Akhmetiev, M.A., Beniamovski, V.N., 2004. Paleocene and Eocene of Western Eurasia (Russian sector)–stratigraphy, palaeogeography, climate. Neues Jahrb. Geol. Palaeontol. Abh. 234, 137–181.
Backman, J., Moran, K., McInroy, D.B., Mayer, L.A., the Expedition 302 Scientists, 2006. Proc. IODP 302. Integrated Ocean Drilling Program Management International, Inc., College Station TX.
Barker, P.R., Kennett, J.P., et al., 1988. Proc. ODP, Init. Repts., 113. Ocean Drilling Program, College Station, TX.
Berner, R.A., Raiswell, R., 1983. Burial of organic carbon and pyrite sulfur in sediments over Phanerozoic time: a new theory. Geochim. Cosmochim. Acta 47, 855–862.
Böttcher, M.E., Brumsack, H.J., Dürselen, C.D., 2007. The isotopic composition of modern seawater sulfate: I. Coastal waters with special regard to the North Sea. J. Mar. Syst. 67 (1–2), 73–82.
Bottrell, S.H., Newton, R.J., 2006. Reconstruction of changes in global sulfur cy-cling from marine sulfate isotopes. Earth-Sci. Rev. 75, 59–83.
Bralower, T.J., Premoli Silva, I., Malone, M.J., et al., 2002. Proceedings of the Ocean Drilling Program, Initial Reports, Site 1211, Leg 198. Ocean Drilling Program, College Station, Texas (81 p).
Breheret, J.-G., Brumsack, H.-J., 2000. Barite concretions as evidence of pauses in sedimentation in the Marnes Bleues Formation of Vocontian Basin (SE France). Sediment. Geol. 130, 205–228.
Burdett, J., Arthur, M., Richardson, M., 1989. A Neogene seawater sulfur isotope age curve from calcareous pelagic microfossils. Earth Planet. Sci. Lett. 94 (3–4), 189–198.
Chambers, L.A., Trudinger, P.A., 1979. Microbiological fractionation of stable sulfur isotopes: a review and critique. Geomicrobiol J. 1, 249–293.
Claypool, G.E., Holser, W.T., Kaplan, I.R., Sakai, H., Zak, I., 1980. The age curve of sulfur and oxygen isotopes in marine sulfate and their mutual interpretation. Chem. Geol. 28, 190–260.
Clementz, M., Bajpai, S., Ravikant, V., Thewissen, J., Saravanan, N., Singh, I., Prasad, V., 2011. Early Eocene warming events and the timing of terrestrial faunal exchange between India and Asia. Geology 39 (1), 15–18.
Coplen, T.B., Hopple, J.A., Böhlke, J.K., Peiser, H.S., Rieder, S.E., Krouse, H.R., Rosman, K.J.R., Ding, T., Vocke Jr., R.D., Révész, K.M., Lamberty, A., Taylor, P., De Bièvre, P., 2002. Compilation of minimum and maximum isotope ratios of selected elements in naturally occurring terrestrial materials and reagents. In: Water Resour. Invest. Rep. U.S. Geol. Surv. 01–4222.
Dean, W.E., Schreiber, B.C., 1977. Authigenic Barite, Initial Reports of Deep Sea Drilling Project Leg 41. U.S. Government Printing Office, Washington, D.C, pp. 915–931.
Dymond, J., Suess, E., Lyle, M., 1992. Barium in deep-sea sediments. A geochemical proxy or paleoproductivity. Paleoceanography 7, 163–181.
Edgar, K.M., Pälike, H., Wilson, P.A., 2013. Testing the impact of diagenesis on the $d^{18}O$ and $d^{13}C$ of benthic foraminiferal calcite from a sediment burial depth transect in the equatorial Pacific. Paleoceanography 28, 468–480.
Fike, D.A., Grotzinger, J.P., 2008. A paired sulfate-pyrite $\delta^{34}S$ approach to understanding the evolution of the Ediacaran–Cambrian sulfur cycle. Geochim. Cosmochim. Acta 72 (11), 2636–2648.
Ganeshram, R.S., Francois, R., Commeau, J., BrownLeger, S.L., 2003. An experimental investigation of barite formation in seawater. Geochim. Cosmochim. Acta 67, 2599–2605.
Garrels, R.M., Lerman, A., 1984. Coupling of the sedimentary sulfur and carbon cy-cles—an improved model. Am. J. Sci. 284, 989–1007.
Gill, B.C., Lyons, T.W., Jenkyns, H.C., 2011. A global perturbation to the sulfur cycle during the Toarcian Oceanic Anoxic Event. Earth Planet. Sci. Lett. 312, 484–496.
Gleason, J.D., Thomas, D.J., Moore Jr., T.C., Blum, J.D., Owen, R.M., Haley, B.A., 2009. Early to middle Eocene history of the Arctic Ocean from Nd–Sr isotopes in fossil fish debris Lomonosov Ridge. Paleoceanography 24, PA2215.
Gradstein, F.M., Ogg, J.G., Schmitz, M., 2012. The Geologic Time Scale 2012. Elsevier, pp. 1176.
Habicht, K.S., Canfield, D.E., 1997. Sulfur isotope fractionation during bacterial sulfate reduction in organic-rich sediments. Geochim. Cosmochim. Acta 61, 5351–5361.
Halas, S., Szaran, J., 2001. Improved thermal decomposition of sulfates to SO_2 and mass spectrometric determinations of $\delta^{34}S$ of IAEA-SO-5, IAEA-SO-6 and NBS-127 sulfate standards. Rapid Commun. Mass Spectrom. 15, 1618–1620.
Halevy, I., Peters, S.E., Fischer, W.W., 2012. Sulfate burial constraints on the Phanerozoic sulfur cycle. Science 337, 331–334.
Heath, G.R., Burekle, L.H., et al., 1985. Init. Repts. DSDP. U.S. Govt. Printing Office, Washington, pp. 86.
Holland, H.D., 2002. Volcanic gases, black smokers, and the Great Oxidation Event. Geochim. Cosmochim. Acta 66 (21), 3811–3826.
Horita, J., Zimmermann, H., Holland, H.D., 2002. Chemical evolution of seawater during the Phanerozoic: Implications from the record of marine evaporites. Geochim. Cosmochim. Acta 66, 3733–3756.
Kampschulte, A., Strauss, H., 2004. The sulfur isotopic evolution of Phanerozoic seawater based on the analysis of structurally substituted sulfate in carbonates. Chem. Geol. 204, 255–286.
Kampschulte, A., Bruckschen, P., Strauss, H., 2001. The Sulphur isotopic composition of trace sulphates in Carboniferous brachiopods: implications for coeval seawater, correlation with other geochemical cycles and isotope stratigraphy. Chem. Geol. 175, 165–189.
Kaplan, I.R., Emery, K.O., Rittenberg, S.C., 1963. The distribution and isotopic abundance of Sulphur in recent marine sediments off southern California. Geochim. Cosmochim. Acta 27, 297–331.
Kurtz, A.C., Kump, L.R., Arthur, M.A., Zachos, J.C., Paytan, A., 2003. Early Cenozoic decoupling of the global carbon and sulfur cycles. Paleoceanography 18, 1090.
Lancelot, Y., Seibold, E., et al., 1978. Init. Repts. DSDP. U.S. Govt. Printing Office, Washington, pp. 41.
Longinelli, A., 1989. Oxygen-18 and sulphur-34 in dissolved oceanic sulphate and phosphate. In: Fritz, P., Fontes, J.C. (Eds.), Handbook of Environmental Isotope Geochemistry. 3. Elsevier, Amsterdam, pp. 219–255.
Lyle, M.W., Wilson, P.A., Janecek, T.R., et al., 2002. Proceeding of the Ocean Drilling Program, Initial Reports. Ocean Drilling Program. Texas A&M University, College Station TX77845–9547, USA, pp. 199 Available from.
Marenco, P.J., Corsetti, F.A., Hammond, D.E., Kaufman, A.J., Bottjer, D.J., 2008. Oxidation of pyrite during extraction of carbonate associated sulfate. Chem.Geol. 247, 124–132.
Markovic, S., Paytan, A., Li, H., Wortmann, U.G., 2016. A revised seawater sulfate oxygen isotope record for the last 4 Myr. Geochim. Cosmochim. Acta 175, 239–251.
Mayer, L., Theyer, F., et al., 1985. Inil. Repts. DSDP. U.S. Govt. Printing Office, Washington, pp. 85.
Mazumdar, A., Goldberg, T., Strauss, H., 2008. Abiotic oxidation of pyrite by Fe(III) in acidic media and its implications for sulfur isotope measurements of lattice-bound sulfate in sediments. Chem. Geol. 253, 30–37.
Moberly, R., Gardner, J.V., Larson, R.L., 1975. Init. Repts. DSDP. U.S. Govt. Printing Office, Washington, pp. 32.
Najman, Y., Appel, E., BouDagher-Fadel, M., Bown, P., Carter, A., Garzanti, E., Godin, L., Han, J.T., Liebke, U., Oliver, G., Parrish, R., Vezzoli, G., 2010. The timing of India–Asia collision: geological, biostratigraphic and palaeomagnetic constraints. J. Geophys. Res. 115, B12416.
Ogawa, Y., Takahashi, K., Yamanaka, T., Onodera, J., 2009. Significance of euxinic condition in the middle Eocene paleo-Arctic basin: a geochemical study on the IODP Arctic coring expedition 302 sediments. Earth Planet. Sci. Lett. 285, 190–197.
Pälike, H., Nishi, H., Lyle, M., Raffi, I., Gamage, K., Klaus, A., the Expedition 320/321 Scientists, 2010. Expedition 320/321 summary. In: Pälike, H., Lyle, M., Nishi, H., Raffi, I., Gamage, K., Klaus, A., the Expedition 320/321 Scientists (Eds.), Proc. IODP, 320/321. Integrated Ocean Drilling Program Management International, Inc, Tokyo.
Paytan, A., Gray, E.T., 2012. Sulfur isotope stratigraphy. In: Gradstain, F.M., Ogg, J.G., Schmitz, M.D., Ogg, G.M. (Eds.), The Geologic Timescale 2012. 1. Elsevier, Boston, USA, pp. 167–180.
Paytan, A., Griffith, E.M., 2007. Marine barite: recorder of variations in ocean export productivity. Deep-Sea Res. II 54, 687–705.
Paytan, A., Kastner, M., Martin, E.E., Macdougall, J.D., Herbert, T., 1993. Marine barite as a monitor of seawater strontium isotope composition. Nature 366, 445–449.
Paytan, A., Kastner, M., Chavez, F.P., 1996. Glacial to interglacial fluctuations in productivity in the equatorial Pacific as indicated by marine barite. Science 274 (5291), 1355–1357.
Paytan, A., Kastner, M., Campbell, D., Thiemens, M.H., 1998. Sulfur isotopic composition of Cenozoic seawater sulfate. Science 282, 1459–1462.
Paytan, A., Mearon, S., Cobb, K., Kastner, M., 2002. Origin of marine barite deposits: Sr and S isotope characterization. Geology 30, 747–750.
Paytan, A., Kastner, M., Campbell, D., Thiemens, M.H., 2004. Seawater sulfur isotope fluctuations in the cretaceous. Science 304, 1663–1665.
Peirce, J., Weissel, J., et al., 1989. Proceedings of the Ocean Drilling Program Initial Report. College Station, Texas A&M University, USA, pp. 121.
Perrin, J., Rivard, C., Vielzeuf, D., Laporte, D., Fonquernie, C., Ricolleau, A., Cotte, M., Floquet, N., 2017. The coordination of sulfur in synthetic and biogenic Mg calcites: the red coral case. Geochim. Cosmochim. Acta 197, 226–244.
Pierre, C., 1985. Isotopic evidence for the dynamic redox cycle of dissolved sulphur compounds between free and interstitial solutions in marine salt pans. Chem. Geol. 53, 191–196.
Present, T.M., Paris, G., Burke, A., Fischer, W.W., Adkins, J.F., 2015. Large carbonate associated sulfate isotopic variability between brachiopods, micrite, and other sedimentary components in Late Ordovician strata. Earth Planet. Sci. Lett. 432, 187–198.
Rennie, V.C.F., Turchyn, A.V., 2014. The preservation of and in carbonate-associated sulfate during marine diagenesis: a 25 Myr test case using marine sediments. Earth Planet. Sci. Lett. 395, 13–23.
Rennie, V.C.F., Paris, G., Sessions, A.L., Abramovich, S., Turchyn, A.V., Adkins, J.F., 2018. Cenozoic record of $\delta^{34}S$ in foraminiferal calcite implies an early Eocene shift to deep-ocean sulfide burial. Nat. Geosci. 11, 761–765.
Richardson, J.A., Newville, M., Lanzirotti, A., Webb, S.M., Rose, C.V., Catalano, J.G., Fike, D.A., 2019. Depositional and diagenetic constraints on the abundance and spatial variability of carbonate-associated sulfate. Chem. Geol. 523, 59–72.
Richter, F.M., Liang, Y., 1993. The rate and consequences of Sr diagenesis in deep-sea carbonates. Earth Planet. Sci. Lett. 117, 553–565.
Rose, C.V., Fischer, W.W., Finnegan, S., Fike, D.A., 2019a. Records of carbon and sulfur cycling during the Silurian Ireviken Event in Gotland, Sweden. Geochim. Cosmochim.

Acta 246, 299–316.
Rose, C.V., Webb, S.M., Newville, M., Lanzirotti, A., Richardson, J.A., Tosca, N.J., Catalano, J.G., Bradley, A.S., Fike, D.A., 2019b. Insights into past ocean proxies from micron-scale mapping of sulfur species in carbonates. Geology 47, 1–5.
Sager, W.W., Winterer, E.L., Firth, J.V., et al., 1993. Proc. ODP, Init. Repts. Ocean Drilling Program, College Station, TX, pp. 143.
Schidlowski, M., Hayes, J.M., Kaplan, I.R., 1983. Isotopic interferences of ancient biochemistry of carbon, sulfur, hydrogen and nitrogen. In: Schopf, J.W. (Ed.), Earth's Earliest Biosphere: Its Origin and Evolution. Princeton University Press, pp. 149–186.
Staudt, W.J., Schoonen, M.A.A., 1995. Sulfate incorporation into sedimentary carbonates. ACS Symp. Ser. 612, 332–345.
Stickley, C.E., St John, K., Koç, N., Jordan, R.W., Passchier, S., Pearce, R.B., Kearns, L.E., 2009. Evidence for middle Eocene Arctic sea ice from diatom sand ice-rafted debris. Nature 460, 376–379.
Strauss, H., 1997. The isotopic composition of sedimentary sulfur through time. Palaeogeogr. Palaeoclimatol. Palaeoecol. 132, 97–118.
Takano, B., 1985. Geochemical implications of sulfate in sedimentary carbonates. Chem. Geol. 49, 393–403.
Taylor, B.E., Ding, T., Halas, S., Breas, O., Robinson, B.W., 2000. Accurate calibration of the V-CDT Scale: proposed d^{34}S values for calibration and reference materials and methods of correction for SO_2-based analyses. In: Report of Sulfur Isotope Working Group 8th Advisory Group Meeting on Future Trends in Stable Isotope Reference Materials and Laboratory Quality Assurance. IAEA, Vienna, Austria.
Torres, M.E., Brumsack, H.J., Bohrmann, G., Emeis, K.C., 1996. Barite fronts in continental margin sediments: a new look at barium remobilization in the zone of sulfate reduction and formation of heavy barites in diagenetic fronts. Chem. Geol. 127, 125–139.
Turchyn, A.V., Schrag, D.P., Coccioni, R., Montanari, A., 2009. Stable isotope analysis of the cretaceous sulfur cycle. Earth Planet. Sci. Lett. 285, 115–123.
Voigt, J., Hathorne, E.C., Frank, M., Vollstaedt, H., Eisenhauer, A., 2015. Variability of carbonate diagenesis in equatorial Pacific sediments deduced from radiogenic and stable Sr isotopes. Geochim. Cosmochim. Acta 148, 360–377.
Walker, J.C.G., 1986. Global geochemical cycles of carbon, sulfur and oxygen. Mar. Geol. 70 (1–2), 159–174.
Wortmann, U.G., Paytan, A., 2012. Rapid variability of seawater chemistry over the past 130 million years. Science 337, 334–336.
Wotte, T., Shields-Zhou, G.A., Strauss, H., 2012. Carbonate-associated sulfate: experimental comparisons of common extraction methods and recommendations toward a standard analytic protocol. Chem. Geol. 326–327, 132–144.
Yao, W., Paytan, A., Wortmann, U.G., 2018. Large-scale ocean deoxygenation during the Paleocene-Eocene Thermal Maximum. Science 361 (6404), 804–806.
Yao, W., Wortmann, U.G., Paytan, A., 2019. Sulfur isotopes—use for stratigraphy during times of rapid perturbations. Stratigraphy & Timescales 4, 1–33.
Yao, W., Paytan, A., Griffith, E.M., Martínez-Ruiz, F., Markovic, S., Wortmann, U.G., 2020. A revised seawater sulfate δ^{34}S curve for the Eocene. Chem. Geol. 532, 119382.
Zachos, J.C., Kroon, D., Blum, P., et al., 2004. Proceedings of the Ocean Drilling Program Initial Report. College Station, Texas A&M University, USA, pp. 208.